Dicle University
Journal of Engineering
https://dergipark.org.tr/tr/pub/dumf
duje.dicle.edu.tr

Research Article

The Effectiveness of Advanced Cooling Solutions in Managing the Thermal Performance of Lithium-Ion Batteries: A Numerical Study

Serhat AYDIN[1*], Metin UZUN[2]

[1] Cevheri Air, Aircraft Body Engine Maintenance Technical Expert, serhat.aydin@cevheriair.com, Orcid No: 0009-0005-4784-5013
[2] Iskenderun Technical University, Department of Airframe and Powerplant Maintenance, metin.uzun@iste.edu.tr, Orcid No 0000-0002-0744-3491

ARTICLE INFO

Article history:

Received 1 February 2025
Received in revised form 27 February 2025
Accepted 6 March 2025
Available online 30 June 2025

Keywords:

Liquid Cooling Systems, Thermal Management, Cooling Channel Design, Lithium-Ion Batteries, Numerical Analysis

DOI: 10.24012/dumf.1631467

* Corresponding author

ABSTRACT

This study explores the advanced thermal management of lithium-ion batteries (LiBs) using a comprehensive Battery Thermal Management System (BTMS) framework. Employing numerical simulations and experimental validations, the research evaluates three distinct cooling configurations (Case 1, Case 2, and Case 3) under varying coolant flow velocities (0.1 m/s, 0.5 m/s, and 1 m/s) and coolant types (water and ethylene glycol). Incorporating nanofluids, the study demonstrates significant improvements in heat transfer efficiency compared to conventional methods. Findings reveal that higher flow velocities enhance heat dissipation and temperature uniformity. Additionally, water outperforms ethylene glycol due to its superior thermal conductivity. A temperature gradient from 298 K to 318 K underscores the importance of optimized flow distribution and channel geometry. This work not only addresses critical challenges in LiB thermal management but also offers significant insights into the design of safer and more efficient cooling systems for applications such as electric vehicles and renewable energy storage. In addition to providing theoretical insights, this research offers actionable recommendations for the design of such systems. Future directions for this research include the integration of microchannel cooling and phase change materials to further enhance thermal performance.

Introduction

Lithium-ion (LiB) batteries have become the standard for modern energy storage systems, powering a wide range of applications, including electric vehicles (EVs), portable electronics, and renewable energy grids [1–4]. This widespread adoption is primarily due to their high energy density, long cycle life, and relatively low self-discharge rate, making them essential to meet the increasing energy demands of modern technologies [5,6]. However, as the energy density of LiBs increases, heat generation during operation also intensifies due to Joule heating and electrochemical reactions, posing critical thermal management challenges [7,8]. Effective thermal regulation is crucial to ensuring battery safety, enhancing performance, and extending operational life [9].

Thermal challenges associated with LiBs include uneven temperature distribution, capacity degradation, and, in extreme cases, thermal runaway, which can lead to catastrophic battery failure [10,11]. To address these issues, Battery Thermal Management Systems (BTMS) have been extensively researched, with liquid cooling methods gaining prominence due to their superior heat transfer efficiency compared to air-cooling systems [12,13].

Recent advancements in BTMS technology have introduced innovative cooling strategies such as microchannel cooling, phase change materials (PCMs), and nanofluid-based cooling [14–16]. Microchannel cooling systems, known for their compact design and high thermal performance, are particularly effective for high-power applications where space is limited [17]. Similarly, PCMs provide a passive cooling solution by absorbing heat during phase transitions, maintaining temperature uniformity [18]. Additionally, nanofluids, which involve dispersing nanoparticles into traditional coolants like water or ethylene glycol, significantly enhance thermal conductivity and overall cooling performance [19].

The design and optimization of cooling channels are crucial for the effectiveness of BTMS. Factors such as channel geometry, spacing, and flow rate directly influence heat dissipation, pressure drop, and energy efficiency [20,21]. Proper channel design not only improves thermal management but also reduces energy consumption, making it particularly valuable for applications such as EVs and grid energy storage systems [22,23].

This study investigates advanced liquid cooling systems for the thermal regulation of LiBs. Through a combination of numerical simulations and experimental validations, various cooling configurations are evaluated to assess their impact on temperature regulation, flow dynamics, and energy efficiency. By examining three distinct cooling channel designs and incorporating nanofluids, this work aims to provide actionable insights for optimizing BTMS and addressing the growing thermal challenges in high-performance battery systems.

Models and Methods

This study offers a novel contribution to battery thermal management systems (BTMS) by systematically investigating three distinct cooling configurations: Case 1, Case 2, and Case 3 channels. Unlike prior research, which often focuses on a single design, this work provides a comparative evaluation of these configurations under varying coolant flow rates using both water and ethylene glycol. The study explores the impact of three inlet velocities (0.1 m/s, 0.5 m/s, and 1 m/s) on the cooling performance, highlighting their influence on heat dissipation, temperature uniformity, and pressure drop. Furthermore, the incorporation of nanofluids in the cooling process distinguishes this study, demonstrating significant improvements in thermal conductivity and overall system efficiency compared to traditional cooling fluids.

By integrating numerical simulations and experimental validations, the research delivers critical insights into the optimization of channel geometry, flow conditions, and coolant properties for BTMS.

Table 1. Specifications of the battery

Density (kg/m3)	2450
Specific heat (J/kg·K)	1108
Thermal conductivity (W/(m·K))	3.9
Heat generated of each LiB (W/m3)	240,000
Initial temperature (K)	298.15
Length (mm)	118
Width (mm)	63
Height (mm)	13
Nominal capacity (Ah)	8
Nominal voltage(V)	3.2
Charge cut-off voltage (V)	3.8
Discharge cut-off voltage (V)	2.1
Coolant thickness (mm)	5

In this study, water and ethylene glycol based coolants commonly used for battery thermal management were preferred. Alternative coolants such as nanofluid doped coolants (e.g. Al_2O_3-water, CuO-water, TiO_2-water) and dielectric coolants (e.g. Novec 7000, Fluorinert) are also known to be used in the literature. However, these alternatives were not included in the study due to their high cost, stability issues such as precipitation and viscosity increase over time, risks of deposition on heat transfer surfaces and limited availability in commercial applications. Although some dielectric fluids used in electric vehicle batteries have low viscosity and high temperature resistance, water-based solutions are safer in terms of sealing requirements and chemical stability. In addition, within the scope of the targeted study, it is aimed to create a model suitable for real-world applications based on commonly used refrigerants in existing commercial systems. Future studies can further investigate the effects of nanofluid additives on heat transfer efficiency and the effect of dielectric fluids and two-phase cooling systems on battery performance.

These findings contribute to the development of safer, more efficient and durable energy storage systems by addressing key challenges in lithium-ion battery heat management. Case 1 consists of 3 batteries and 2 coolers, Case 2 consists of 2 batteries and 2 coolers, and finally Case 3 consists of 3 batteries and 4 coolers. The cooler length and width are the same as the battery size, but its thickness is taken as 5 mm in this study. Three different designs were tested in this study to evaluate how different fluids can maintain battery temperatures at an optimal level.

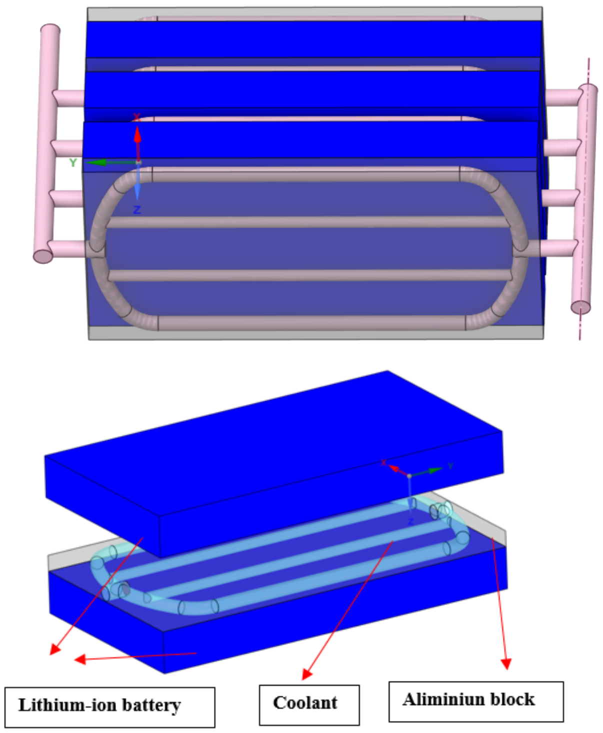

Figure 1. Schematic diagram of BTMS.

Figure 1 illustrates the schematic design of the BTMS, showing the main components, including cooling channels, battery cells, and heat dissipation pathways. In the context of a Battery Thermal Management System (BTMS), the fluid can be considered incompressible as the velocity of the coolant is significantly lower than the speed of sound. The Reynolds number, one of the main criteria used to determine the flow regime, is related to the viscosity, density, velocity and characteristic length of the fluid. In the Honeycomb Liquid Cooling Plate (HLCP), the flow regime is determined by the dynamic viscosity of the refrigerant and the geometric properties of the cooling plate.

The flow regime is classified in three different cases:
Laminar flow: If the Reynolds number is below 2300, the flow is smooth and stratified. Transitional regime: If the Reynolds number is between 2300 and 4000, the flow starts to become irregular. Turbulent flow: If the Reynolds number is above 4000, swirling and irregular flow characteristics are observed.

This classification is critical to understanding how the coolant moves across the surface of the coil. While turbulent flow in particular can provide more effective cooling by increasing the heat transfer coefficient, it can cause excessive pressure losses. The equation used to calculate the Reynolds number is given in Equation (1) (Qian et al., 2016). Figure 1 presents a schematic representation of the cooling structure designed for the Battery Thermal Management System (BTMS). The main components of the system include lithium-ion battery modules, refrigerant channels and an aluminum block for heat dissipation.

The aluminum block is designed to improve heat transfer and thermal uniformity through direct contact with the battery cells. The coolant circulates between the inlet and outlet, transferring heat away from the battery modules. Figure 1 shows a general outline of how the refrigerant flows through the channels, while Figure 2 shows the more detailed internal structure and flow characteristics of the system.

This structure aims to effectively direct the refrigerant and ensure homogeneous temperature distribution on the battery surface. In particular, flow rates, channel design and material selection play a critical role in the safety and performance of the batteries.

$$\mathrm{Re} = \frac{V \bullet d_h}{\mu} \tag{1}$$

The Reynolds number (Re) is a dimensionless quantity that determines the flow regime in a fluid system. It is defined as the ratio of inertial forces to viscous forces and is calculated using the equation.

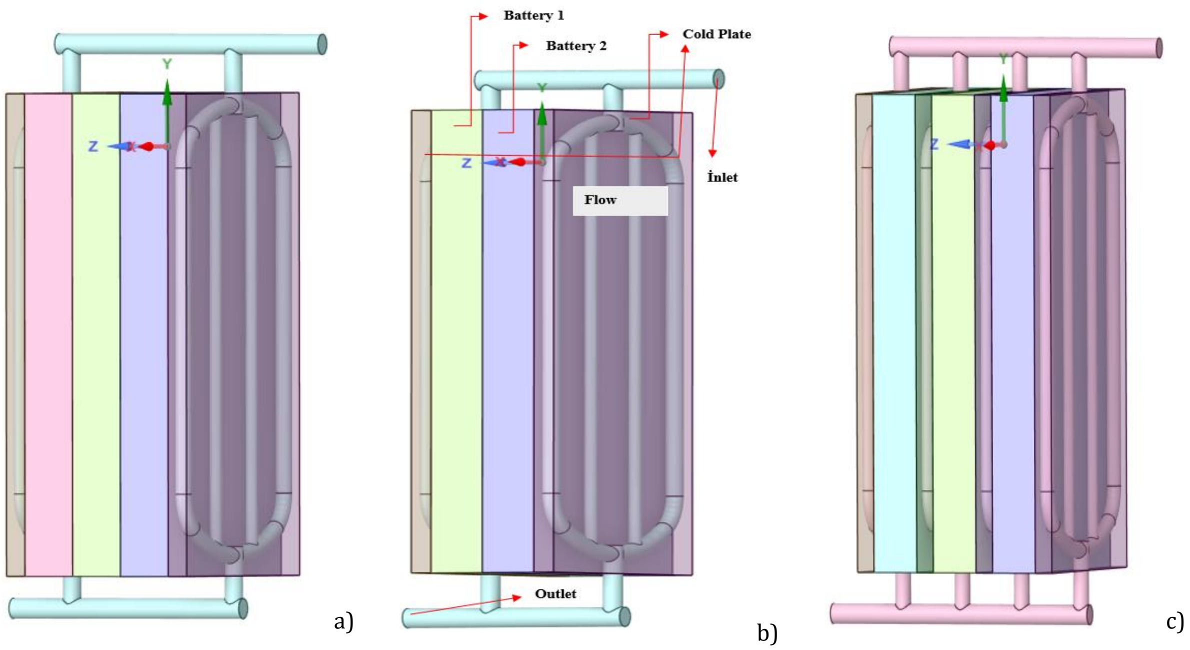

Figure 2. The structure of the battery thermal management (a-Case 1, b-Case 2, c-Case 3)

The flow rate of coolant through the Honeycomb Liquid Cooling Plate (HLCP) is denoted by V, the hydraulic diameter of the coolant channel is denoted by dh, and the kinematic viscosity of the coolant is denoted by μ. In battery cooling systems, the flow regime is a fundamental parameter that determines the efficiency of the heat transfer mechanism. The flow regime is determined by the Reynolds number (Re) and can be analyzed in three different regimes: laminar, transitional and turbulent flow. In this study, different flow rates using water and ethylene glycol Reynolds numbers for 0.1m/s, 0.5m/s, 1.0m/s) were calculated. The results obtained are summarized in the table below:

Table 2. Reynolds Number and Flow Regime Classification for Different Fluids and Velocities

Fluid	Hydraulic Diameter (mm)	Viscosity (μ) (Pa·s)	Density (ρ) (kg/m³)	Flow Velocity (m/s)	Reynolds Number (Re)	Flow Regime
Water	5	0,000897	998,2	0,1	557	Laminar
Water	5	0,000897	998,2	0,5	2785	Transitional
Water	5	0,000897	998,2	1	5570	Turbulent
Ethylene Glycol	5	0,015	1111,4	0,1	2000	Transitional
Ethylene Glycol	5	0,015	1111,4	0,5	10000	Turbulent
Ethylene Glycol	5	0,015	1111,4	1	20000	Turbulent

The flow regime in battery cooling systems varies depending on the flow velocity, and while laminar flow is observed at low speeds, as the speed increases, the transition regime and then turbulent flow regime emerges. Especially at speeds of 0.5 m/s and above, turbulence effects become evident. In this study, the SST k-ω turbulence model is preferred because it provides accurate solutions at low Reynolds numbers and accurately models the transition regime. While this model produces more accurate solutions in the low Reynolds region by using the k-ω model near the wall, it switches to the k-ε model in free flow regions and represents the turbulent flow in a wider region. The simulations show that laminar flow is dominant at 0.1 m/s, but the turbulence effect becomes significant at 0.5 m/s and 1.0 m/s. Especially at 1.0 m/s, turbulence is observed to increase the heat transfer coefficient and make the temperature distribution on the battery surface more homogeneous. Therefore, the SST k-ω model is considered as a suitable model for thermal analysis of battery cooling systems because it accurately predicts the transition from laminar to turbulent, captures wall effects well at low velocities, and realistically simulates turbulent flow at high velocities.

$$\frac{\partial}{\partial \tau}(\rho_W C_W T_W) = \nabla \bullet (k_W \nabla T_W) \tag{2}$$

In this context, ρ_W T_W, k_W and C_W which represent the density, temperature, thermal conductivity and specific heat of the water is shown in equation 2.

$$\frac{\partial}{\partial \tau}(\rho_B C_B T_B) = -\nabla \bullet (k_B \nabla T_B) + Q_B \tag{3}$$

The parameters ρ_B C_B T_B and k_B represent the density, specific heat capacity, temperature, and thermal conductivity of the lithium-ion battery, respectively. Additionally, Q_B denotes the heat generation rate of a single lithium-ion battery. The energy conservation equation of lithium-ion battery is shown (Qian et al., 2016) in equation (3). This equation assumes that heat transfer occurs mainly via conduction and that radiation effects are negligible. The thermal model considers an unsteady (transient) state, as the battery temperature changes over time due to charge and discharge cycles. For this study, the internal heat generation rate was taken as 240,000 W/m³, which is consistent with experimental findings in similar research (Qian et al., 2016). The equation helps determine the temperature distribution in battery cells, which directly impacts cooling system design by optimizing heat dissipation pathways and preventing thermal runaway.

Table 1 presents key specifications for the battery, including its density (2450 kg/m³), specific heat (1108 J/kg·K), and thermal conductivity (3.9 W/m·K), which are crucial for understanding the battery's heat generation and thermal management needs. The battery generates significant heat (240,000 W/m³), and its relatively low thermal conductivity means that an efficient cooling system is essential to prevent overheating. The physical dimensions of the battery (118 mm length, 63 mm width, 13 mm height) further define the available surface area for heat dissipation, while the 5 mm coolant thickness plays a role in cooling effectiveness. Table 3 provides properties of the materials used for thermal management, including an aluminum block with a high thermal conductivity (238 W/m·K), which helps dissipate heat from the battery efficiently. Water, with a high specific heat (4182 J/kg·K) but lower thermal conductivity (0.6 W/m·K), is used as a coolant to absorb heat, while ethylene glycol offers a balance of density (1111.4 kg/m³) and thermal conductivity (0.252 W/m·K) for effective heat transfer in various thermal systems.

The battery thermal properties used in the study are based on the properties of widely used lithium-ion cells. The parameters used in the simulations, such as thermal conductivity, heat capacity and heat generation rate, were determined based on lithium-ion battery cells that are frequently referenced in the literature. However, in order to improve the accuracy of the model, the specific characteristics of the battery type used are detailed and the boundary conditions are clearly defined. Heat generation is modeled based on battery charge and discharge rates, and surface boundary conditions are determined by considering natural convection and forced convection effects due to the cooling fluid. In this framework, additional explanations are provided in the relevant section for a clearer understanding of the thermal properties and boundary conditions.

Table 3. Properties of the employed materials.

Thermo-physical properties	Aluminum block	Water	ethylene-glycol
Density (kg/m3)	2700	998.2	1111.4
Specific heat (J/kg·K)	900	4182	2415

Thermal conductivity (W/(m·K))	238	0.6	0.252

Table 3 presents the thermo-physical properties of the materials employed for thermal management, including aluminum, water, and ethylene glycol. Aluminum, with a density of 2700 kg/m³ and a thermal conductivity of 238 W/m·K, is used primarily for heat dissipation due to its high thermal conductivity, making it highly effective at transferring heat away from the battery. Water, with a density of 998.2 kg/m³ and a specific heat of 4182 J/kg·K, plays a vital role as a coolant due to its ability to absorb and store a significant amount of thermal energy, although its lower thermal conductivity (0.6 W/m·K) means it requires efficient flow design to transfer heat effectively. Ethylene glycol, with a density of 1111.4 kg/m³ and a thermal conductivity of 0.252 W/m·K, is used for its favorable properties in cooling systems, offering a balance between fluid density and heat transfer characteristics, particularly in lower temperature environments or when a lower freezing point is required.

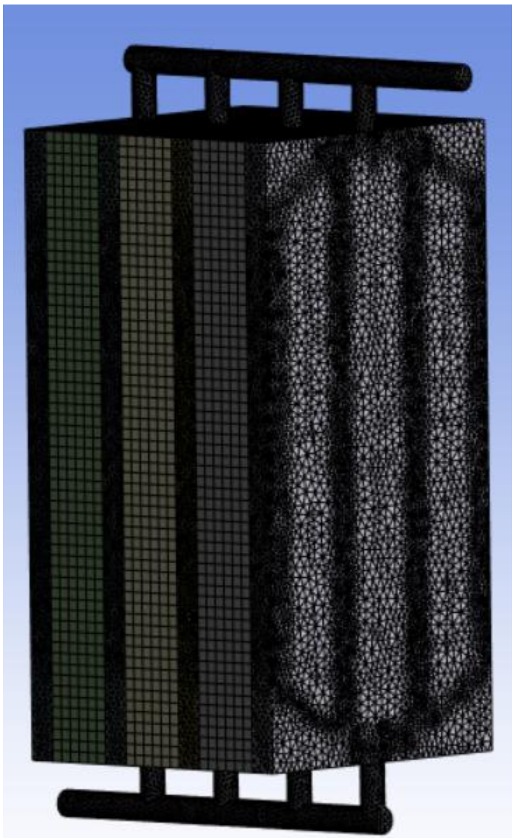

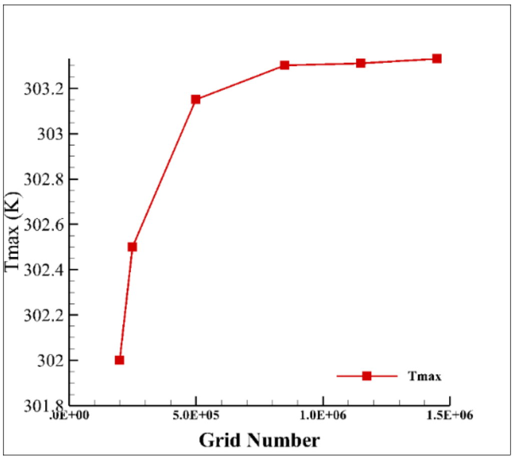

Figure 3. Meshing method.

The computational fluid dynamics (CFD) model, boundary conditions and assumptions used in the study are clearly defined. The Shear Stress Transport (SST) k-ω model is used for turbulence modeling, which is preferred because it produces accurate results at low Reynolds numbers and captures the transition regime accurately. In the simulations, wall functions were applied to accurately represent the flow in turbulent regions.

A mesh independence test was performed to evaluate the effect of the mesh resolution on the results. As part of the mesh independence test, the number of elements was varied from 300,000 to 1,500,000 and the maximum battery surface temperatures were compared. After 750,000 elements, the variation in temperature values dropped below 0.2%, so the final simulations were performed with a 750,000 element network structure, taking into account the balance of computational cost and accuracy. Numerical simulations were performed in ANSYS Fluent software and an irregular tetrahedral mesh structure was used to optimize accuracy and computational efficiency. In order to capture in detail the flow dynamics and thermal variations in the cooling ducts, the mesh element size was set to 1 mm. Thinner elements are used in areas where heat exchange is intense, especially on the walls of the cooling channels. In terms of mesh quality, the orthogonal quality is 0.257 and the maximum skewness is 0.74, which are within acceptable limits in terms of solution accuracy.

The results of the network independence test show that once the network resolution reaches a certain level (750,000 elements), its effect on the results becomes negligible. After 1,000,000 elements, the rate of temperature change reaches 0.05% and it is determined that using a higher resolution mesh increases the computation time but contributes minimally to the results. Therefore, considering the balance of computation time and accuracy, the optimal mesh resolution was determined as 750,000 elements.

Table 4. The results of the network independence test are given in the table below:

Mesh Element Sayısı	Tmax (K)	Fark (%)
300,000	302.1	-
500,000	303.0	0.9%
750,000	303.2	0.2%
1,000,000	303.25	0.05%
1,500,000	303.27	0.01%

These results clearly show that the effect of mesh resolution on the solution becomes negligible after 750,000 elements. Thus, computation time is optimized while ensuring simulation accuracy.

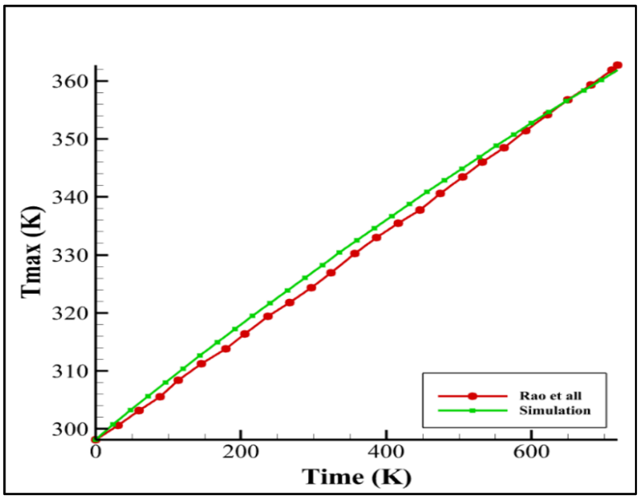

Figure 4. Validation of the heat generation model.

The validity of the heat generation model was established through a comparative analysis of simulation outputs and experimental data, yielding an error margin of no more than 5%. This figure shows the temperature profiles of the battery surface under a heat generation rate of 240,000 W/m³, demonstrating consistent agreement between numerical predictions and experimental observations. Validation confirms the model's ability to accurately represent lithium-ion battery thermal behavior during operation.

Conclusion and Discussion

In this section, the results of the thermal and flow analyses of the cooling system are presented and discussed. The visualization of temperature and velocity distribution across the battery pack and coolant channels provides insights into the effectiveness of the implemented cooling strategies. The following figures illustrate how variations in coolant flow rates, coolant types, and the positioning of the batteries influence the overall thermal performance of the system. These results highlight key factors such as the temperature gradient across the battery pack, the impact of coolant flow velocity on heat dissipation, and the differences in performance between water and ethylene glycol as coolants. The discussion focuses on identifying potential design improvements, optimizing flow distribution, and enhancing cooling efficiency to ensure safe and efficient operation of the battery system.

Results of case 1

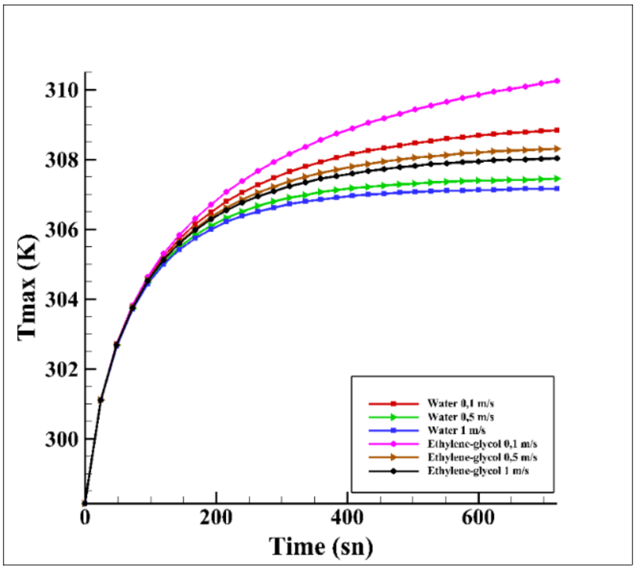

Figure 5. Coolant water and ethylene glycol at different fluid velocities for Case 1

Figure 5 shows the battery temperature distribution for three different coolant flow rates (0.1 m/s, 0.5 m/s and 1 m/s) and two different coolant types (water and ethylene glycol). The results reveal that increasing the flow rate decreases the temperature of the battery. At 0.1 m/s, higher temperature values are observed, while cooling becomes more efficient at higher speeds. In particular, when water was used as the coolant, the temperature reached about 308.15 K at 0.1 m/s and decreased to 303.15 K at 1 m/s. When ethylene glycol was used, the temperature was around 307.15 K at 0.1 m/s and decreased to about 301.15 K at 1 m/s.

These results show that both the flow rate and the type of coolant play an important role in battery heat dissipation.

Although ethylene glycol has lower thermal conductivity compared to water, more efficient heat transfer was achieved at higher flow rates, resulting in larger temperature drops. However, higher flow rates also mean increased pump power requirements, which can affect system efficiency. Therefore, determining the optimum coolant type and flow rate in battery thermal management systems is a critical factor in terms of both thermal performance and energy consumption.

Figure 6 presents a comprehensive representation of the temperature and velocity distributions within the cooling system. On the left side, the overall battery pack is displayed, followed by individual battery temperature profiles, highlighting the variations in thermal behavior due to the batteries' positions. The first battery, closest to the coolant inlet, exhibits the lowest temperature, while the last battery, positioned near the outlet, reaches the highest temperature due to reduced cooling efficiency along the flow path. Below the battery pack, the coolant temperature distribution is shown, indicating a steady increase from the inlet to the outlet, reflecting the heat absorption as the coolant moves through the system. The coolant velocity is also visualized, with a clear decrease in velocity from the inlet to the outlet due to frictional losses and the design of the cooling channels. This analysis underscores the importance of optimizing both temperature and flow distribution to enhance the cooling performance and thermal management of the battery pack.

Table 5. Temperature and velocity distribution in the battery cooling system for Case 1, including maximum and minimum cell temperatures for different coolant types and flow velocities.

	Fluid Type	Water			Ethylene-glycol		
	Fluid Velocity	0,1 m/s	0,5 m/s	1 m/s	0,1 m/s	0,5 m/s	1 m/s
Cell 1	Tmax (K)	305,22	304,11	303,92	306,44	304,82	304,59
Cell 2		305,24	304,12	303,927	306,45	304,83	304,6
Cell 1	Tmin(K)	299,27	298,62	298,48	300,53	299,26	299,11
Cell 2		299,39	298,66	298,52	300,56	299,3	299,11

The table 5. shows the maximum (Tmax) and minimum (Tmin) temperature values for different coolant types (water and ethylene-glycol) and varying flow rates (0.1 m/s, 0.5 m/s, 1 m/s) in the battery cells for Case 1. The results show that increasing the flow rate decreases the Tmax values of the coils and decreases the Tmin values to lower levels, making the temperature distribution more balanced. Water provides a more efficient cooling by providing lower Tmax and Tmin values, while ethylene-glycol shows a higher but more stable temperature distribution. Especially high Tmax values pose a critical risk to the thermal safety of batteries, while balancing Tmin levels reduces the temperature difference between cells and improves battery performance. These data show that optimal flow rate and coolant selection in battery cooling systems play an important role in preventing battery overheating and extending battery life by stabilizing operating temperatures.

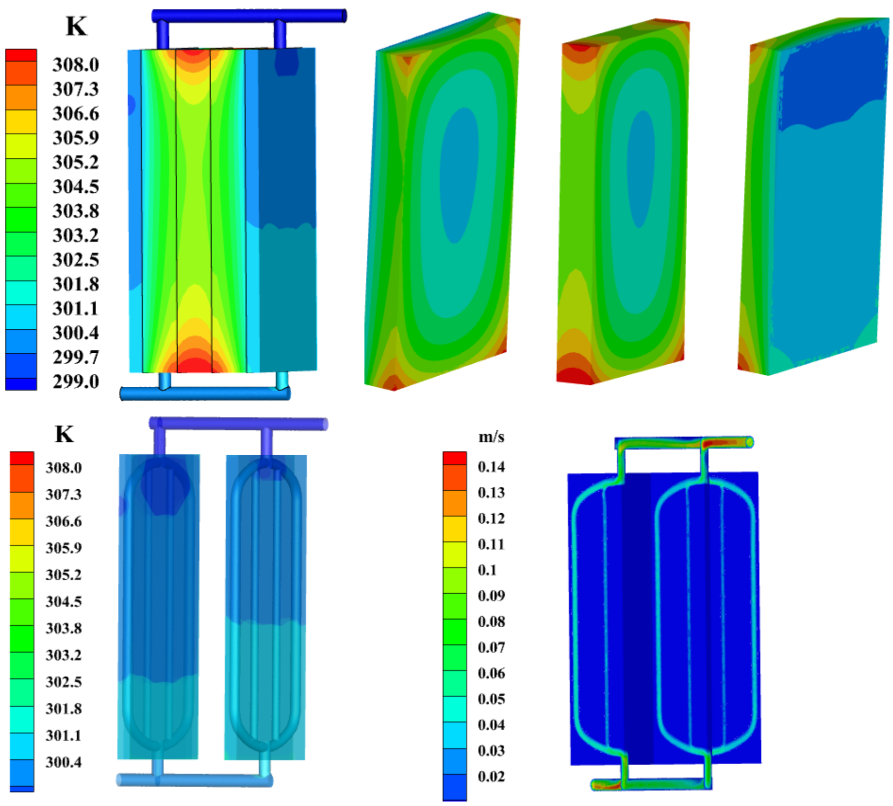

Figure 6. Temperature and speed distribution of battery, coolant and fluid for case 1

Figure 6 visually presents the temperature and velocity distribution in the battery pack, refrigerant and liquid for Case 1. In the Case 1 configuration, there are 3 batteries and 2 heat sinks and in this structure, the refrigerant enters at the designated inlet point, circulates between the batteries and leaves the system at the outlet point.Battery surface temperature distribution: The surface temperatures of the coils change with the flow of the fluid, with the coils in the inlet zone having lower temperatures and the coils near the outlet having higher temperatures. This can be explained by the fact that the coolant absorbs heat as it travels and its temperature increases towards the outlet. Refrigerant velocity variation: While the fluid velocity is highest in the inlet zone (inlet), the velocity decreases as it moves through the ducts due to wall friction and pressure losses and reaches lower values in the outlet zone (outlet). In narrow ducts, local variations in velocity can be observed due to flow diversion, which can affect the heat transfer between the coils.

Results of case 2

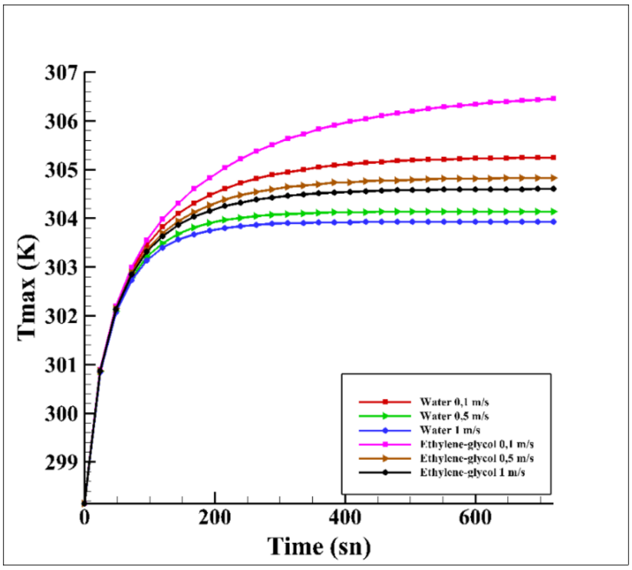

Figure **7.** Coolant water and ethylene glycol at different fluid velocities for Case 2

Temperature distribution of the coolant: As the coolant comes into contact with the batteries, it absorbs heat and its temperature increases. The temperature increase is more pronounced especially in the outlet region of the battery modules, which necessitates optimization of the cooling channel design to ensure a homogeneous temperature distribution on the battery surface. Cooling channel design and flow direction: The figure visualizes the layout of the cooling channels and the path of the fluid. It shows in detail how the fluid is directed from the inlet to the outlet and how the cooling process takes place.This analysis shows that higher flow rates provide more homogeneous temperature distribution over the battery surface, but local temperature differences occur at lower rates. As the glycol, depending on the fluid velocity (0.1 m/s, 0.5 m/s and 1 m/s). As the refrigerant velocity increases, a significant decrease in the battery temperature is observed for both refrigerants. At 0.1 m/s, the temperature remains at higher levels, especially for ethylene glycol, which has a lower thermal conductivity.

When water is used, the battery temperature reaches about 308.15 K at 0.1 m/s and drops to about 303.15 K at 1 m/s. Similarly, with ethylene glycol, the temperature is about 307.15 K at 0.1 m/s and decreases to about 301.15 K at 1 m/s. The results show that higher flow rate increases heat dissipation, resulting in a more homogeneous temperature distribution. Although ethylene glycol has lower thermal conductivity compared to water, the increased flow rate compensates for this disadvantage, resulting in larger temperature drops. However, localized hot spots can occur at low flow rates, which can adversely affect the long-term lifetime of the battery. These results highlight the importance of optimizing the coolant type and flow rate in battery thermal management and show that it is critical to minimize the thermal stress on battery cells.

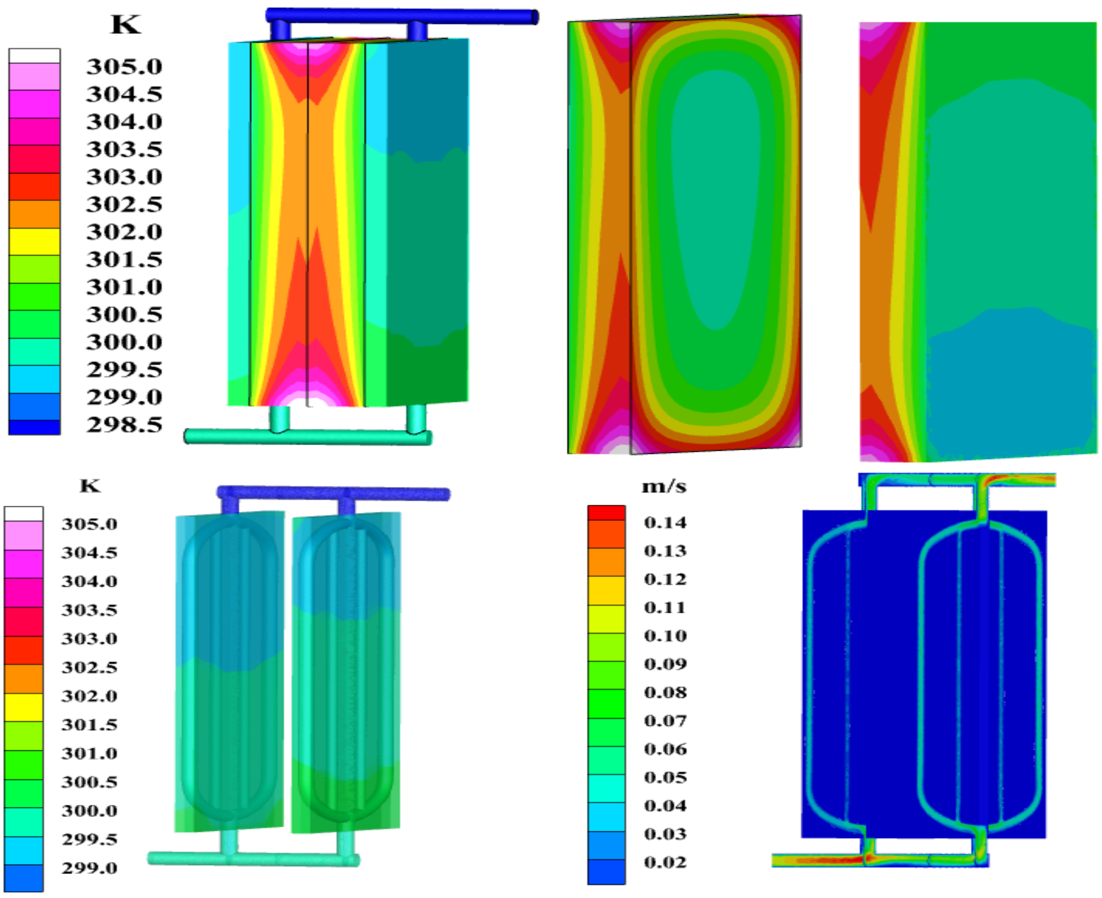

Figure 8. Temperature and speed distribution of battery, coolant and fluid for case 2

Table 6 shows the effect of different coolant types (water and ethylene-glycol) and varying flow rates (0.1 m/s, 0.5 m/s, 1 m/s) on the maximum (Tmax) and minimum (Tmin) temperature values in the battery cells in the battery cooling system for Case 2. The results show that water provides more effective cooling for the batteries with lower Tmax and Tmin values. While Tmax values decrease with increasing flow rate, Tmin values create a more balanced temperature distribution. Although the Tmax values of ethylene-glycol are higher compared to water, the temperature change is more stable and the temperature differences between the cells are relatively reduced. This highlights the critical role of fluid type and velocity on temperature control in battery thermal management.

Table 6. Temperature and velocity distribution in the battery cooling system for Case 2, including maximum and minimum cell temperatures for different coolant types and flow velocities.

	Fluid Type	Water			Ethylene-glycol		
	Fluid Velocity	0,1 m/s	0,5 m/s	1 m/s	0,1 m/s	0,5 m/s	1 m/s
Cell 1	Tmax (K)	307,9	306,51	306,23	309,41	307,42	307,15
Cell 2		308	306,57	306,29	309,43	307,46	307,16
Cell 3		308,83	307,43	307,15	310,23	308,31	308
Cell 1	Tmin (K)	299,79	298,91	298,7	301,46	299,78	299,58
Cell 2		299,97	299	298,79	301,51	299,84	299,59
Cell 3		300,76	299,68	299,45	302,16	300,5	300,28

Figure 8 presents a detailed analysis of the temperature and velocity distributions within the cooling system. On the left side, the overall battery pack is shown, followed by the individual batteries placed within the system. Each battery's temperature is depicted separately, illustrating the thermal behavior based on its position within the pack. The first battery, closest to the coolant inlet, maintains the lowest temperature, while the last battery, near the outlet, experiences the highest temperature due to decreased cooling efficiency as the coolant travels through the system.

Below the battery pack, the coolant temperature distribution is shown, indicating the progressive increase in temperature as the coolant moves along the cooling channels. The velocity distribution of the coolant is also presented, illustrating how the flow speed varies from the inlet to the outlet, with the coolant velocity gradually decreasing as it flows through the system. This visualization emphasizes the importance of flow optimization to ensure even temperature distribution and effective cooling throughout the battery pack.

Results of case 3

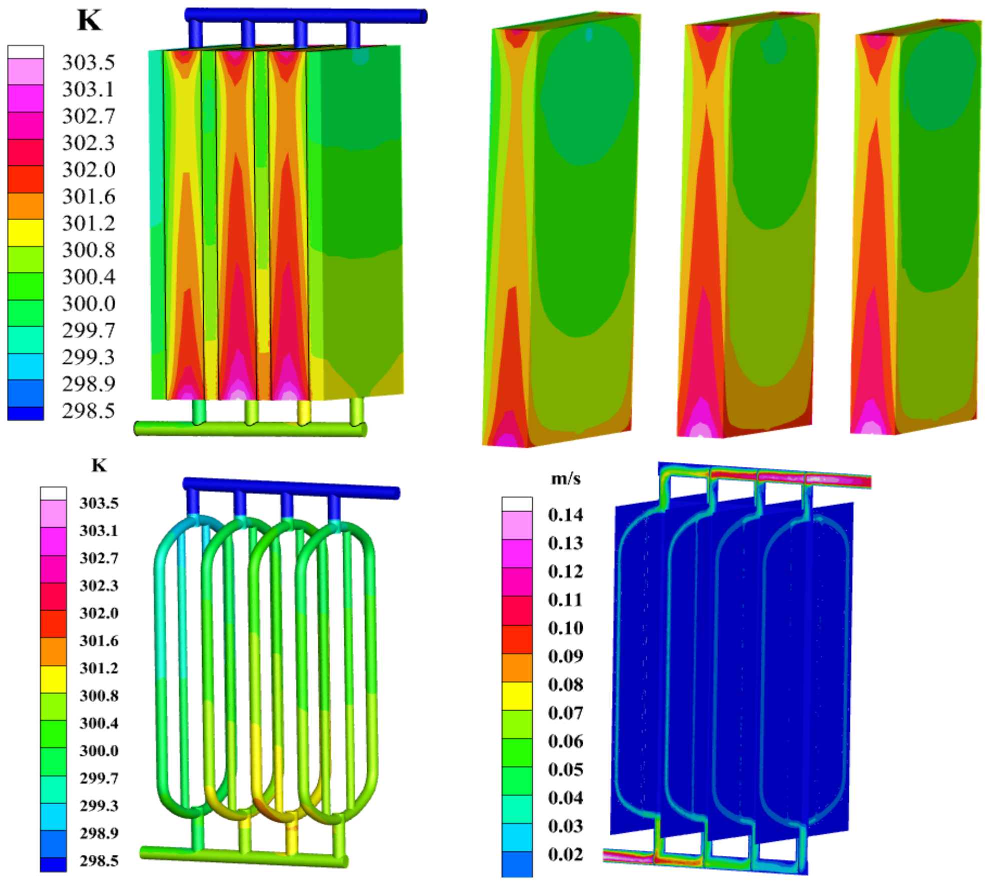

Figure 9. Temperature and speed distribution of battery, coolant and fluid for case 3

Figure 9 presents in detail the temperature and velocity distribution in the battery cooling system and compares the thermal performance of different fluids (water and ethylene glycol) at various flow rates. In the figure, the battery pack overview is on the left side and the temperature profiles of the batteries are presented on the right side. It can be clearly observed how the temperature distribution changes depending on the location of the coils in the system.

When the temperature distribution in the cooling system is examined, it is seen that the temperature of the battery close to the inlet point is at the lowest level, while the temperature increases as it approaches the outlet point. This increase can be explained by the fact that the refrigerant absorbs heat as it progresses and its temperature rises towards the outlet. Especially when ethylene glycol is used, the temperature increase at the outlet point is more pronounced and it is confirmed that it has a lower heat transfer capacity compared to water. The figure also shows the velocity profile of the refrigerant. While the fluid velocity is highest in the inlet region, it is observed that the velocity decreases towards the outlet due to friction and pressure drop on the channel walls. This may affect the cooling performance and cause temperature differences on the battery surface. Especially at low speeds, it is observed that the coils in the outlet area cannot be cooled sufficiently.

The thermal performances of water and ethylene glycol at different speeds are also compared in the figure. Due to its high thermal conductivity, water provides more efficient cooling of the coils, especially at high flow rates. In contrast, ethylene glycol has a low thermal conductivity, which keeps the temperature of the batteries at higher levels under the same conditions. At low flow rates (0.1 m/s), there is no significant temperature difference between the two fluids, but when the flow rate is increased to 1.0 m/s, the superiority of water in cooling performance becomes clearer.

This analysis shows that not only thermal conductivity but also operating conditions, freezing point and fluid viscosity should be taken into account when selecting the optimum refrigerant for battery cooling systems. Figure 9 shows how the battery temperature distribution varies with factors such as fluid selection and flow rate, providing a critical decision point in engineering design.

Table 7. Temperature and velocity distribution in the battery cooling system for Case 3, including maximum and minimum cell temperatures for different coolant types and flow velocities.

	Fluid Type	Water			Ethylene-glycol		
	Fluid Velocity	0,1 m/s	0,5 m/s	1 m/s	0,1 m/s	0,5 m/s	1 m/s
Cell 1	Tmax (K)	303,33	301,47	301,11	304,49	302,21	301,71
Cell 2		303,39	301,53	301,21	304,78	302,38	301,85
Cell 3		302,85	301,24	301,033	304,44	302,08	301,59
Cell 1	Tmin (K)	299,73	298,6	298,42	300,822	299,19	298,87
Cell 2		299,73	298,65	298,49	301,31	299,42	299,04
Cell 3		299,22	298,43	298,35	301,25	299,05	298,76

Table 7 shows the temperature variations in the battery cells for Case 3. When water was used, the Tmax values ranged from 303.33 K to 301.11 K, while when ethylene-glycol was used, they were measured between 304.49 K and 301.71 K. As the flow rate increased, Tmax decreased while Tmin values became more stable. In terms of Tmin, water presented values between 299.22 K and 298.42 K, while ethylene-glycol presented values between 301.25 K and 298.76 K. Water provides a more effective cooling with lower maximum temperature values, while ethylene-glycol offers a higher but more stable temperature distribution.

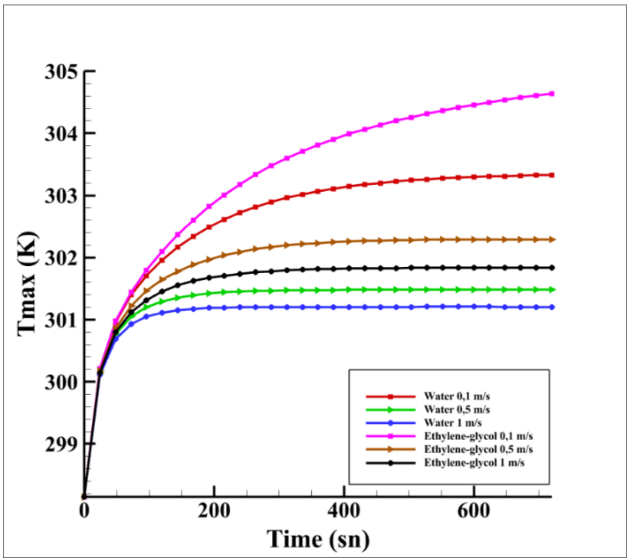

Figure 10. Coolant water and ethylene glycol at different fluid velocities for Case 3

Figure 10 illustrates the temperature variation of the battery with respect to the coolant flow velocity (0.1 m/s, 0.5 m/s, and 1 m/s) and two different types of coolants: water and ethylene glycol. The analysis shows a clear inverse relationship between flow velocity and temperature. As the coolant flow velocity increases, the temperature of the battery decreases due to more effective heat removal. For water, the temperature at 0.1 m/s reaches approximately 309.15 K, but it decreases to around 303.15 K at a flow velocity of 1 m/s. In contrast, for ethylene glycol, the temperature is slightly higher than water at all velocities. At 0.1 m/s, the battery temperature is about 308.15 K, while it reduces to 302.15 K at 1 m/s. These results highlight that despite water having a better heat dissipation capacity due to its higher thermal conductivity, both coolants benefit from higher flow velocities in reducing battery temperature, with water consistently providing better thermal management.

In order to evaluate the accuracy of the numerical model presented in this study, comparisons were made with experimental studies in the literature [24] investigated the effect of cyclic heat pipe and graphite sheet inserts on the cooling performance of a new generation battery thermal management system for electric vehicles. The data obtained in this study are comparable to the findings presented by our numerical model in terms of battery temperature control. Similarly, Chen et al [25] evaluated the effectiveness of a symmetric air-cooled system on battery thermal management and analyzed in detail how the flow channel structure affects the temperature distribution. Furthermore, another study [26] investigated how the battery pack structure can be optimized to improve the cooling efficiency of parallel air-cooled battery management systems.

The model presented in the present study shows a high level of agreement in terms of temperature distribution and cooling efficiency when compared with the experimental findings in the aforementioned literature. The turbulence model and heat transfer calculation methods used in the numerical analysis are consistent with the techniques proposed in the literature and support the reliability of the model. In this context, the findings are in line with previous studies on battery thermal management systems.

In order to increase the practical applicability of the study and emphasize the impact of the results in real-world scenarios, the following points can be addressed:

The battery thermal management system analyzed in this study can be used in a wide range of applications such as electric vehicles, energy storage systems and industrial power systems. Since overheating of batteries in electric vehicles can lead to both performance loss and safety risks, the developed cooling system can optimize the battery temperature and provide a safer and longer life. It can also be used to reduce the effects of heat build-up during fast charging, thus improving battery charging efficiency.

In terms of energy storage systems, temperature control is a critical factor in electricity storage systems supplied from renewable energy sources. Especially in lithium-ion battery-based energy storage facilities, temperature differences can cause imbalances between battery modules, leading to capacity loss. The liquid-cooled thermal management system proposed in this study can prolong battery life and improve system reliability by ensuring temperature uniformity in such energy storage applications.

However, the constraints and challenges in practical applications of the system must also be addressed. First of all, the design and integration of the cooling system needs to take into account the additional weight and volume it can add. Since the size and weight of the battery pack in electric vehicles directly affects energy efficiency, the cooling circuit needs to be optimized to be lightweight and compact. Furthermore, pump and liquid circulation systems can increase energy consumption, so the design of the system should balance between optimal cooling performance and minimum energy consumption.

In conclusion, the thermal management system developed in this study offers significant advantages for electric vehicles, energy storage systems and industrial applications, and has the potential to extend battery life, especially in scenarios requiring fast charging and long-term use. However, factors such as cost, design optimization and energy consumption need to be taken into account for the commercial applicability of the system.

Conclusion

This study comprehensively analyzed the thermal and flow characteristics of a battery thermal management system (BTMS) used in lithium-ion batteries (LiBs), considering different coolant types (water and ethylene glycol) and flow velocities (0.1 m/s, 0.5 m/s, and 1 m/s). The results demonstrated that the temperature distribution within the battery pack is highly sensitive to both the coolant flow rate and the type of coolant employed. As the coolant flow velocity increased, there was a noticeable decrease in the battery temperature, indicating that higher flow rates contribute to more efficient heat dissipation. Water, with its higher thermal conductivity, was found to be more effective in reducing the temperature of the batteries, particularly at higher flow velocities, compared to ethylene glycol. Ethylene glycol, despite its lower thermal conductivity and higher exit temperature, still performed reasonably well, albeit with slightly higher temperatures than water, particularly at lower flow velocities.

The temperature gradient observed within the battery pack ranged from 298 K at the coolant inlet to 318 K at the outlet, highlighting the need for optimizing the flow distribution to prevent thermal hotspots. The analysis revealed that while the coolant temperature increased along the flow path, the temperature rise was more pronounced when ethylene glycol was used instead of water, indicating the need to consider coolant properties in the design phase. Furthermore, the velocity distribution of the coolant showed a decrease from the inlet (1 m/s) to the outlet (0.3 m/s), primarily due to frictional losses and the geometry of the cooling channels. This velocity reduction can affect the efficiency of the cooling process and emphasizes the importance of optimizing channel design to minimize friction and maintain effective coolant flow.

The results highlight how coolant flow rate and type significantly affect battery thermal management efficiency. A careful balance between flow rate, coolant type, and channel geometry is essential for maintaining uniform cooling across the entire battery pack, thereby improving the overall performance and lifespan of the system. The results also suggest that future improvements could focus on further optimizing the flow channel geometries to reduce friction losses and enhance flow uniformity. Additionally, exploring advanced cooling techniques, such as microchannel or phase change material (PCM) cooling, could further enhance thermal management efficiency. Long-term studies on the performance of these cooling systems under varying operating conditions would also provide valuable insights into the sustainability and reliability of the system over time.

In conclusion, this study provides valuable data on the importance of cooling system design in battery thermal management. By optimizing the coolant flow velocity, type, and channel design, significant improvements in battery temperature control and system efficiency can be achieved, contributing to safer, more durable, and higher-performing energy storage solutions.

In this study, a liquid cooling system for battery thermal management is analyzed and different battery configurations and hybrid cooling solutions can be evaluated in the future. In particular, hybrid cooling systems based on a combination of air and liquid cooling offer an important alternative to optimize thermal management of batteries and improve energy efficiency. Hybrid systems can reduce energy consumption by utilizing liquid cooling at high power demands and supplemented with air cooling at lower loads. Furthermore, the impact of different battery pack configurations on thermal performance can be studied. Modular battery systems can offer a more flexible structure in terms of thermal management and the effect of different battery cell configurations on temperature uniformity can be investigated. In addition, the potential advantages of phase change materials (PCMs) and nanofluid doped refrigerants on thermal management can be evaluated. PCMs can provide a passive cooling mechanism against sudden temperature spikes of batteries, reducing temperature fluctuations and extending battery life. Nanofluid doped coolants can increase the efficiency of the cooling system by increasing the heat transfer capacity.

In future work, battery thermal management strategies can be further optimized through experimental validation and real-world applications. The proposed cooling system can be tested in electric vehicles (EVs) under real driving conditions to evaluate its impact on battery lifetime, fast charging efficiency and overall energy consumption. It can also be applied in large-scale energy storage systems to analyze its thermal stability and operational safety during variable power demands. To improve the accuracy of the study, future research should include experimental validation with prototype battery packs and compare simulation results with actual temperature distributions. Hybrid cooling systems combining liquid and air cooling can be investigated to optimize energy efficiency, while AI-assisted cooling algorithms can be developed to dynamically adjust coolant flow according to battery load conditions. These developments will ensure that battery cooling technologies are reliable and scalable not only in simulation but also in real-world applications.

Ethics committee approval and conflict of interest statement

There is no need to obtain permission from the ethics committee for the article prepared. There is no conflict of interest with any person / institution in the article prepared.

References

[1] J. M. Tarascon and M. Armand, "Issues and challenges facing rechargeable lithium batteries," Nature, vol. 414, no. 6861, pp. 359–367, 2001,

[2] S. Megahed and B. Scrosati, "Lithium-ion rechargeable batteries," *Journal of Power Sources*, vol. 51, no. 1–2, pp. 79–104, 1994,

[3] A. Pesaran, "Battery thermal management in EVs and HEVs: Issues and solutions," in *Advanced Automotive Battery Conference*, Las Vegas, Nevada, USA, pp. 34–49, 2001.

[4] X. Feng, M. Ouyang, X. Liu, L. Lu, Y. Xia, and X. He, "Thermal runaway mechanism of lithium-ion battery for electric vehicles: A review," *Energy Storage Materials*, vol. 10, pp. 246–267, 2018,

[5] G. Li, "Promotion of practical technology of the thermal management system for cylindrical power battery," *Energy Informatics*, vol. 7, no. 1, p. 33, 2024,

[6] J. Ren, X. Wang, Y. Zhao, and L. Chen, "Battery thermal management system by employing different phase change materials with SWCNT nanoparticles to obtain better battery cooling performance," *Case Studies in Thermal Engineering*, vol. 61, p. 104987, 2024.

[7] S. Argade and A. De, "Optimization study of a Z-type airflow cooling system of a lithium-ion battery pack," *Physics of Fluids*, vol. 36, no. 6, 2024,

[8] M. Hajialibabaei, M. M. Saghir, and M. Z. Saghir, "A critical review of the straight and wavy microchannel heat sink and the application in lithium-ion battery thermal management," *International Journal of Thermofluids*, vol. 14, p. 100153, 2022.

[9] V. V. Tyagi, S. C. Kaushik, S. K. Tyagi, and T. Akiyama, "Development of phase change materials based microchannel thermal management system for high heat flux electronic devices," *Renewable and Sustainable Energy Reviews*, vol. 15, no. 3, pp. 1373–1391, 2011.

[10] Ortiz, Y., Arévalo, P., Peña, D., & Jurado, F. (2024). Recent advances in thermal management strategies for lithium-ion batteries: a comprehensive review. Batteries, 10(3), 83.

[11] H. Jeon, J. Kim, S. Lee, S. H. Lee, and J. H. Park, "Cooling strategy optimization of cylindrical lithium-ion battery pack via multi-counter cooling channels," *Energies*, vol. 16, no. 23, p. 7860, 2023.

[12] Ahmadian-Elmi, M., & Zhao, P. (2024). Review of thermal management strategies for cylindrical lithium-ion battery packs. Batteries, 10(2), 50.

[13] Kurre, S. K., Arya, S., & Yadav, J. (2024). Thermal analysis of batteries of electrical vehicle battery for effective thermal management. Materials Today: Proceedings, 99, 63-69.

[14] Xu, H., Zhang, X., Xiang, G., & Li, H. (2021). Optimization of liquid cooling and heat dissipation system of lithium-ion battery packs of automobile. Case Studies in Thermal Engineering, 26, 101012.

[15] Garud, K. S., Tai, L. D., Hwang, S. G., Nguyen, N. H., & Lee, M. Y. (2023). A review of advanced cooling strategies for battery thermal management systems in electric vehicles. Symmetry, 15(7), 1322.

[16] Wu, C., Sun, Y., Tang, H., Zhang, S., Yuan, W., Zhu, L., & Tang, Y. (2024). A review on the liquid cooling thermal management system of lithium-ion batteries. Applied Energy, 375, 124173.

[17] Zhang, J., Shao, D., Jiang, L., Zhang, G., Wu, H., Day, R., & Jiang, W. (2022). Advanced thermal management system driven by phase change materials for power lithium-ion batteries: A review. Renewable and Sustainable Energy Reviews, 159, 112207.

[18] Son, Y. W., Kang, D., & Kim, J. (2023). Passive battery thermal management system for an unmanned aerial vehicle using a tetrahedral lattice porous plate. Applied Thermal Engineering, 225, 120186.

[19] Mali, V., Saxena, R., Kumar, K., Kalam, A., & Tripathi, B. (2021). Review on battery thermal management systems for energy-efficient electric vehicles. Renewable and Sustainable Energy Reviews, 151, 111611.

[20] Qian, Z., Li, Y., & Rao, Z. (2016). Thermal performance of lithium-ion battery thermal management system by using mini-channel cooling. Energy Conversion and Management, 126, 622-631.

[21] Rahmani, A., Dibaj, M., & Akrami, M. (2024). Recent advancements in battery thermal management systems for enhanced performance of Li-ion

batteries: A comprehensive review. Batteries, 10(8), 265.

[22] Maknikar, S. K., & Pawar, A. M. (2023). Application of phase change material (PCM) in battery thermal management system (BTMS): A critical review. Materials Today: Proceedings.

[23] Ye, J., Aldaher, A. Y. M., & Tan, G. (2023). Thermal performance analysis of 18,650 battery thermal management system integrated with liquid-cooling and air-cooling. Journal of Energy Storage, 72, 108766.

[24] M. Bernagozzi, A. Georgoulas, N. Miché, C. Rouaud, M. Marengo, Novel battery thermal management system for electric vehicles with a loop heat pipe and graphite sheet inserts, Applied Thermal Engineering, 194 (2021), 117061.

[25] K. Chen, Y. Chen, Y. She, M. Song, S. Wang, L. Chen, Construction of effective symmetrical air-cooled system for battery thermal management, Applied Thermal Engineering, 166 (2020), 114679.

[26] K. Chen, M. Song, W. Wei, S. Wang, Design of the structure of battery pack in parallel air-cooled battery thermal management system for cooling efficiency improvement, International Journal of Heat and Mass Transfer, 132 (2019), 309–321.